Electronic Supporting Information for:

Cubic *versus* hexagonal – effect of host crystallinity on the T_1 shortening behaviour of $NaGdF_4$ nanoparticles

Nan Liu,[a] Riccardo Marin,[a] Yacine Mazouzi,[a‡] Greg O. Cron,[b,c,d] Adam Shuhendler,[a,e]

and Eva Hemmer *[a,f]

a. Department of Chemistry and Biomolecular Sciences, University of Ottawa, 10 Marie Curie St. Ottawa (ON) K1N 6N5, Canada.

b. Department of Medical Imaging, The Ottawa Hospital, 501 Smyth Rd. Ottawa (ON) K1H 8L6, Canada.

c. Department of Radiology, University of Ottawa, 501 Smyth Rd. Ottawa (ON) K1H 8L6, Canada.

d. Ottawa Hospital Research Institute, 501 Smyth Rd. Ottawa (ON) K1H 8L6, Canada.

e. University of Ottawa Heart Institute, 40 Ruskin St. Ottawa (ON) K1Y 4W7, Canada.

f. Centre for Advanced Materials Research (CAMaR), University of Ottawa, Ottawa (ON) K1N 6N5, Canada.

‡ *Current Address: Sorbonne Université, Laboratoire de Réactivité de Surface (LRS) UMR7197 CNRS, 4 Place Jussieu - 75005, Paris, France*

*Corresponding Author
E-mail: ehemmer@uottawa.ca

Table of content

Fourier transform infrared (FTIR) spectroscopy

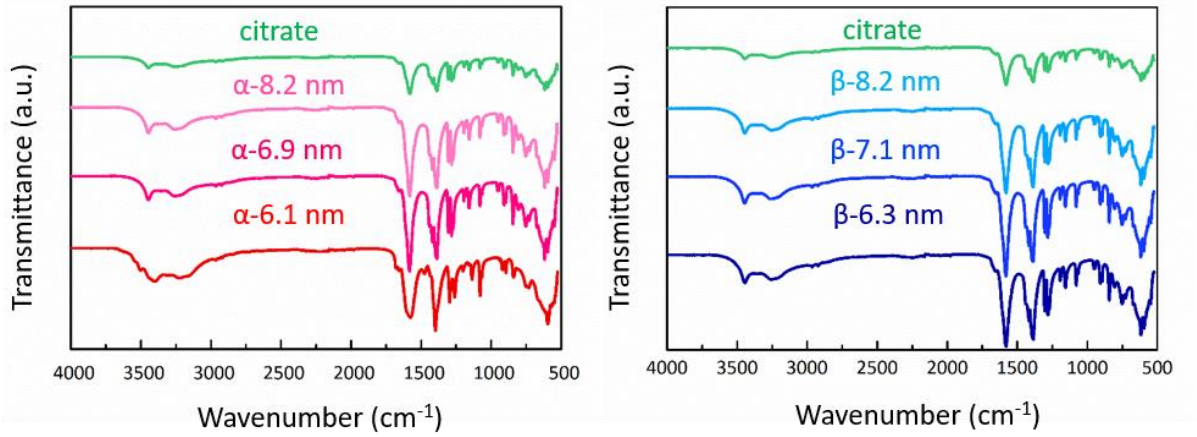

Figure S1. FTIR spectra of citrate-coated cubic (α) and hexagonal (β) $NaGdF_4$ nanoparticles of three different sizes as well as sodium citrate dihydrate used as reference.

The FTIR spectra of both cubic and hexagonal $NaGdF_4$ nanoparticles (NPs) exhibited bands at 3400 and 1600 cm^{-1} that correspond to the stretching and asymmetric stretching vibrations of –OH and $–COO^-$ groups in citrate (F. Carniato, K. Thangavel, L. Tei and M. Botta, *J. Mater. Chem. B*, 2013, **1**, 2442-2446). This indicated successful coating of all samples with citrate molecules.

TEM images of citrate-coated NPs

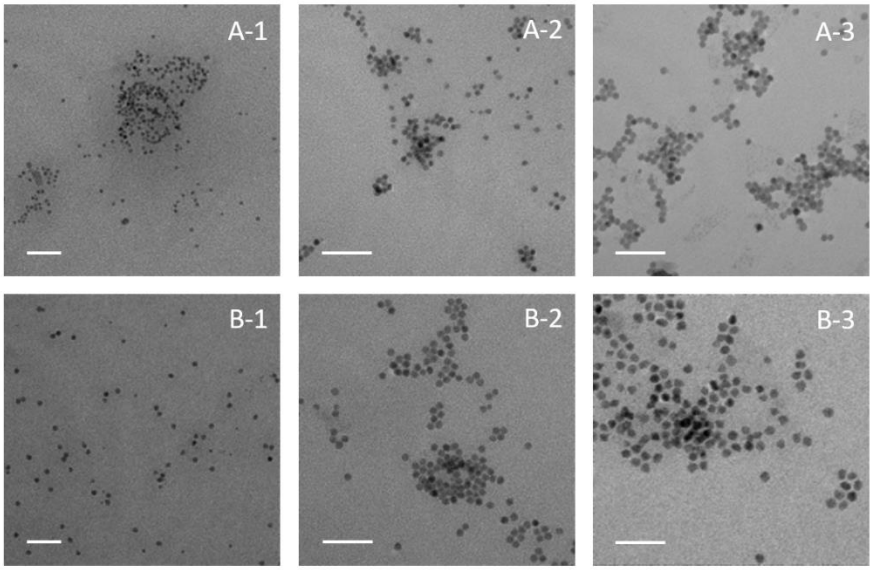

Figure S2. TEM images of citrate-coated $NaGdF_4$ NPs crystallized in the (A) cubic and (B) hexagonal polymorph of three different sizes (6, 7, and 8 nm). Scale bars are 50 nm.

MRI T_2 relaxivity curves

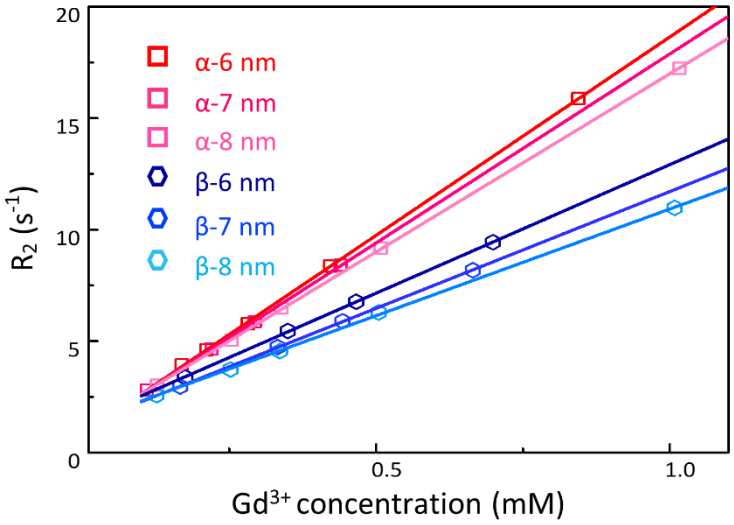

Figure S3. Relaxation rate R_2 (= $1/T_2$) of water protons plotted against the molar concentration of Gd^{3+} for cubic and hexagonal polymorphs of three different NP sizes at 3 T (citrate coating). Red data and fits stand for cubic NPs, while blue data and fits stand for hexagonal NPs.

Dynamic light scattering (DLS) measurements

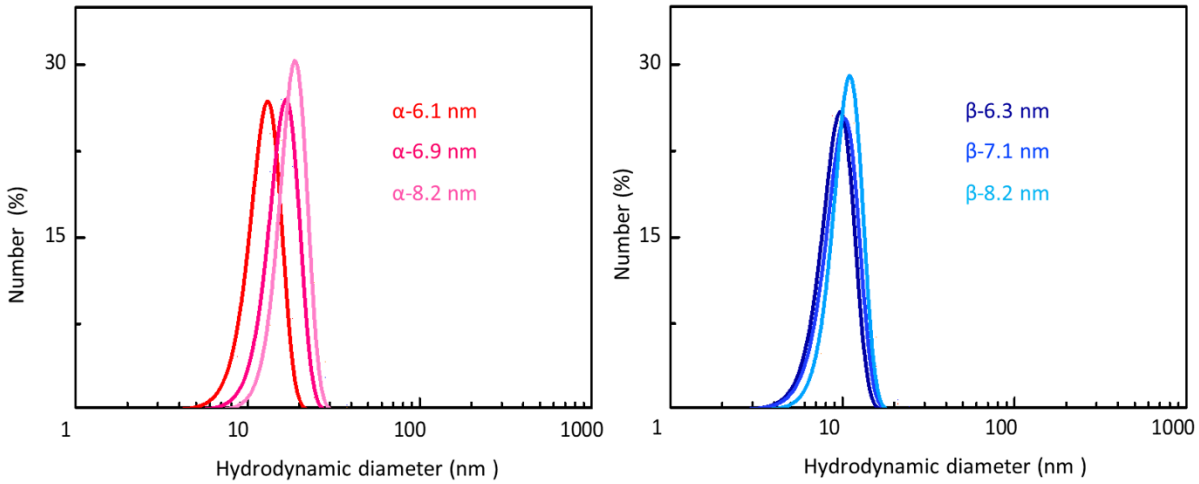

Figure S4. DLS curves of citrate-coated cubic (α) and hexagonal (β) $NaGdF_4$ NPs dispersed in 0.02 M citrate solution. These number-weighted DLS size distributions provide information about the size of those NPs that constitute the major part of the dispersion. Overall, DLS plots, ζ-potential results (Table 1, main manuscript) and TEM observations (Figure S2) confirmed the good dispersibility of all samples.

Thermogravimetric analysis (TGA)

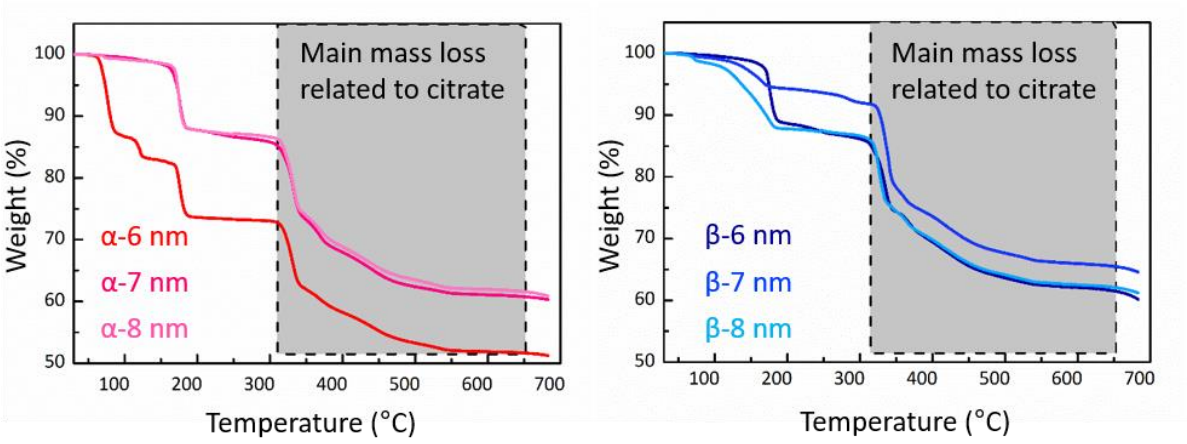

Figure S5. TGA profiles of cubic (α) and hexagonal (β) $NaGdF_4$ NPs collected in air atmosphere.

Estimation of the total number of Gd^{3+} surface ions for cubic and hexagonal NPs

Details, including applied formulas, for the estimation of the total number of Gd^{3+} surface ions are shown in Figure S6 and Table S1. Considering the higher density of the hexagonal polymorph when compared to the cubic, a hexagonal-phase NP contains a larger number of Gd^{3+} ions than a cubic NP of the same size. Consequently, in case of a hexagonal NP, a larger number of Gd^{3+} ions should be available on the surface of the NP to interact with the protons in the surrounding water, thus, yielding a more pronounced T_1 contrast effect. Yet, this is in contrast to our experimental MRI data. This discrepancy can be ascribed to the fact that the overall Gd^{3+} ion concentration of a sample is commonly considered when plotting R_1 as a function of Gd^{3+} ion concentration. Indeed, it was estimated that the overall number of Gd^{3+} surface ions (the contribution of which to T_1 contrast enhancement is more significant than the one of Gd^{3+} ions in the NP volume) does not show any significant difference for cubic and hexagonal $NaGdF_4$ (Table S1 – last row – and Figure S7). These estimations took into account NP sizes as determined *via* TEM, crystallographic data of hexagonal and cubic $NaGdF_4$ derived from XRD PDF cards, and Gd^{3+} ion concentrations in the realm of those obtained by ICP-OES yielding the total number of NPs in each sample. Subsequently, the overall surface and the total number of Gd^{3+} surface ions could be calculated (considering as "surface" of each NP a layer thick enough to contain one unit cell, *i.e.* 0.5 nm). As obvious from Figure S7, the slopes of the curves obtained using the formulas given in Table S1 were very similar for cubic and hexagonal polymorphs. In fact, when the NP size increased to 8 nm, the curves for both polymorphs perfectly overlapped. This indicates that dispersions containing cubic or hexagonal $NaGdF_4$ NPs have very similar total numbers of Gd^{3+} surface ions. Consequently, the number of Gd^{3+} ions as a function of the crystal structure can be ruled out as sole parameter causing the observed differences in r_1.

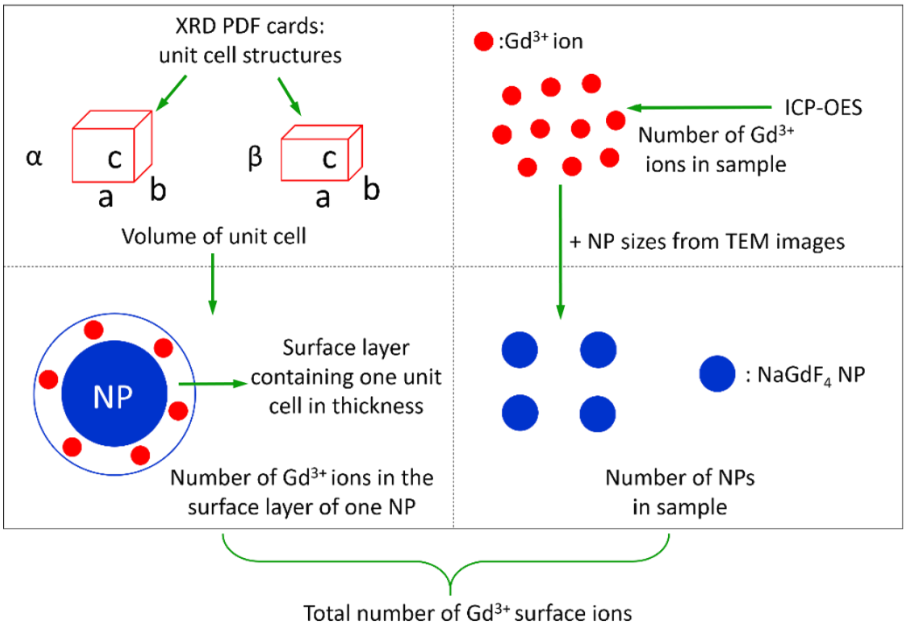

Figure S6. Schematic representation for the estimation of the total number of Gd^{3+} surface ions.

Table S1. Calculation of the total number of Gd^{3+} surface ions in cubic and hexagonal $NaGdF_4$ NPs.

	Formulas	Cubic $NaGdF_4$			Hexagonal $NaGdF_4$		
XRD PDF card number		00-027-0697			01-080-8787		
Number of Gd^{3+} per stoichiometric formula, $N_{Gd/formula}$		1 ($NaGdF_4$)			1.5 [$(NaGdF_4)_{1.5}$]		
Number of formulas, Z		2			1		
a (nm)		0.552			0.603		
b (nm)		0.552			0.603		
c (nm)		0.552			0.361		
Volume of unit cell, V_{cell} (nm^3)	$V_{cell} = a \times b \times c$	0.168			0.113		
Diameter of NP, d (nm)		6.1	6.9	8.2	6.3	7.1	8.2
Volume of NP, V_{NP} (nm^3)	$V_{NP} = \frac{4}{3}\pi\left(\frac{d}{2}\right)^3$	118.85	172.01	288.70	130.92	187.40	288.70
Surface of NP, S_{NP} (nm^2)	$S_{NP} = \pi d^2$	116.9	149.57	211.24	124.69	158.37	211.24
Thickness of NP shell†, dR (nm)	$dR = 0.5$ 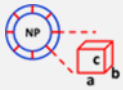						
Volume of shell, V_{shell} (nm^3)	$V_{shell} = \frac{4}{3}\pi\left[\left(\frac{d}{2}\right)^3 - \left(\frac{d}{2} - dR\right)^3\right]$	49.39	64.47	93.26	52.97	68.55	93.26
Number of Gd^{3+} in one NP, $N_{Gd/NP}$	$N_{Gd/NP} = \frac{V_{NP}}{V_{cell}} \times Z \times N_{Gd/Formula}$	1415	2048	3437	1727	2472	3808
Number of Gd^{3+} in the shell of one NP (~ Gd^{3+} surface ions per NP), $N_{Gd/shell}$	$N_{Gd/shell} = \frac{V_{shell}}{V_{cell}} \times Z \times N_{Gd/Formula}$	588	767	1110	699	904	1230
Gd^{3+} concentration determined by ICP-OES‡, C_{mass} (ppm or mg/L)		100	100	100	100	100	100
Gd^{3+} molar concentration, C_{Gd} (mmol/L)	$C_{Gd} = \frac{C_{mass}}{M_{Gd}}$	0.64	0.64	0.64	0.64	0.64	0.64
Total number of Gd^{3+}, N_{Gd} ($\times 10^{20}$/L)	$N_{Gd} = C_{Gd} \times 6.022 \times 10^{23} mol^{-1}$	3.83	3.83	3.83	3.83	3.83	3.83

Table S1 (continued). Calculation of the total number of Gd^{3+} surface ions in cubic and hexagonal $NaGdF_4$ NPs.

	Formulas	Cubic $NaGdF_4$			Hexagonal $NaGdF_4$		
Total number of NPs, N_{NP} ($\times 10^{17}$/L)	$N_{NP} = \frac{N_{Gd}}{N_{Gd/NP}}$	2.71	1.87	1.11	2.22	1.55	1.01
Total number of Gd^{3+} surface ions, $N_{Gd/surface}$ ($\times 10^{20}$/L)	$N_{Gd/surface} = N_{Gd/shell} \times N_{NP}$	1.64	1.48	1.28	1.60	1.45	1.28

† 0.5 nm were chosen as approximate dimension of the unit cells yielding a one-unit-cell thick surface layer.
‡ For each type of NPs, five dispersions with different NP concentrations were analysed by ICP-OES. Yet, here, exemplarily calculations are provided for a concentration of 100 ppm. Identical calculations can be performed for any concentration, including those concentrations obtained by ICP-OES on the samples under investigation, in order to obtain the curves plotted in Figure S7.

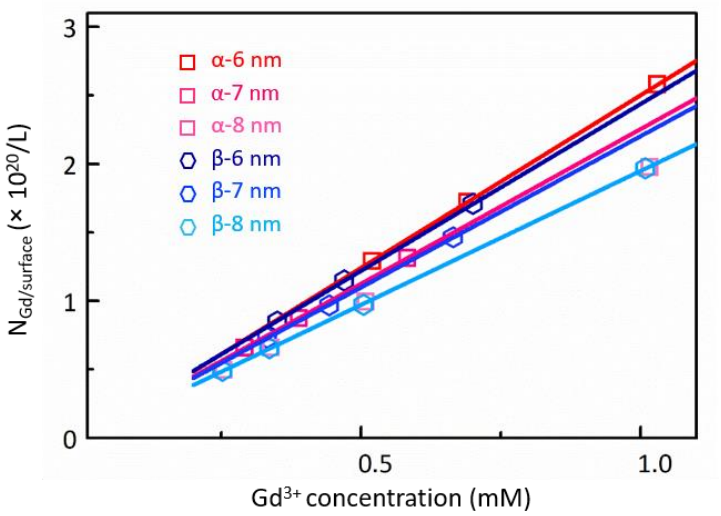

Figure S7. Calculated total number of Gd^{3+} surface ions plotted against the Gd^{3+} molar concentration for cubic and hexagonal polymorphs of three different sizes. Red data points and curves stand for cubic NPs, while blue data points and curves stand for hexagonal NPs (data points represent samples investigated in this study). Note that that the two curves obtained for the largest set of NPs perfectly overlap.

Estimation of citrate mass m_{cit} on the surface of one nanoparticle for cubic and hexagonal polymorphs

Table S2. Estimated citrate mass on the surface of one $NaGdF_4$ nanoparticle (m_{cit}/NP).

	Formulas	Cubic $NaGdF_4$			Hexagonal $NaGdF_4$		
NP diameter, d (nm)		6.1	6.9	8.2	6.3	7.1	8.2
Volumetric mass density, ρ (gcm^{-3})		5.06	5.06	5.06	5.61	5.61	5.61
Mass of one $NaGdF_4$ NP, m_{NP} ($\times 10^{-16}$ mg)	$m_{NP} = \rho \times V_{NP}$	6.02	8.71	14.62	7.34	10.51	16.20
Overall mass of citrate, m_{cit} (mg), based on TGA		1.76	1.92	1.23	1.50	2.12	1.13
Overall mass of NPs, m_{NPs} (mg), based on TGA		4.19	4.63	3.03	3.68	5.04	2.79
Number of NPs, N_{NPs} ($\times 10^{16}$)	$N_{NPs} = \frac{m_{NPs}}{m_{NP}}$	0.70	0.53	0.21	0.50	0.48	0.17
Citrate mass on the surface of one NP, m_{cit}/NP ($\times 10^{-16}$ mg)	$m_{cit}/NP = \frac{m_{cit}}{N_{NPs}}$	2.53	3.61	5.92	3.00	4.43	6.56

Effect of the crystalline phase on r_1 using poly(acrylic acid) as surface ligand

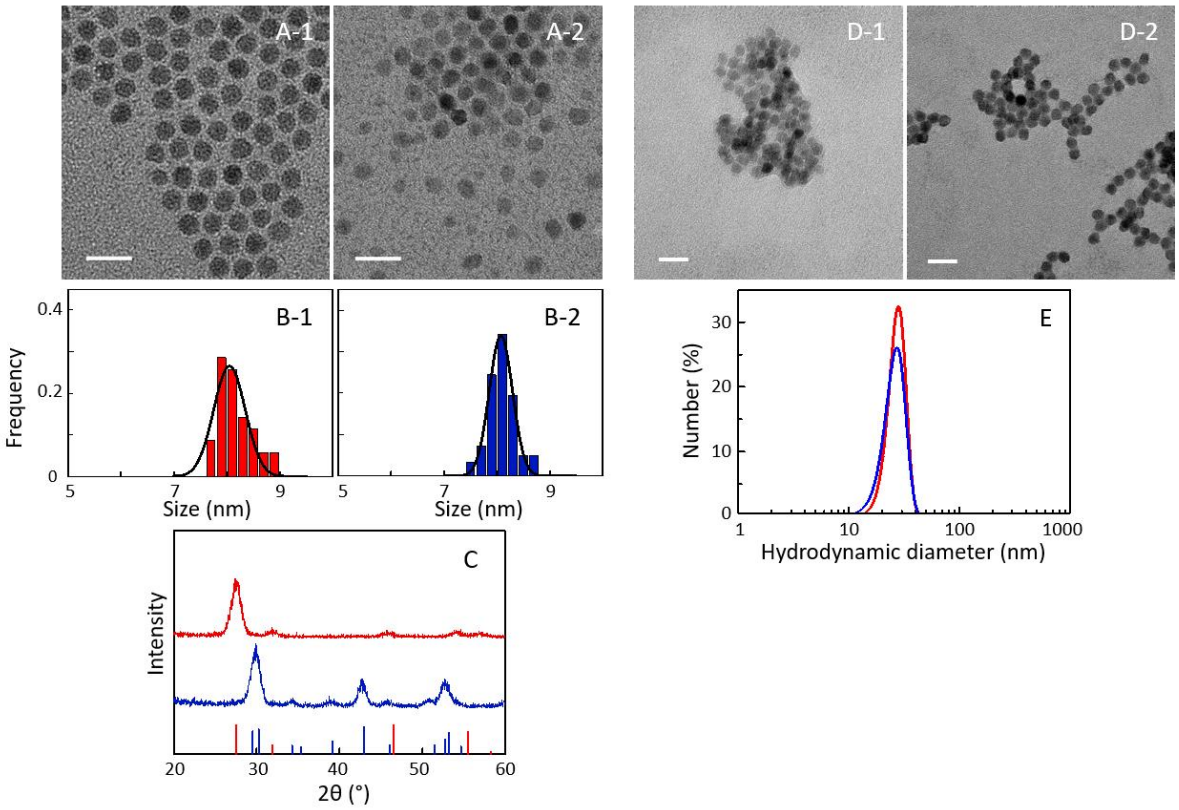

Figure S8. (A) TEM images (scale bars: 20 nm) and (B) size distribution histograms of oleate-coated cubic (1, red) and hexagonal (2, blue) $NaGdF_4$ NPs used for surface modification with poly(acrylic acid) (PAA). Particle sizes of 8.1 ± 0.3 nm and 8.1 ± 0.2 nm were determined for the cubic and the hexagonal phase, respectively. (C) XRD patterns of cubic and hexagonal oleate-capped $NaGdF_4$ NPs. References: red line – cubic $NaGdF_4$ (PDF card no. 00-027-0697), blue line – hexagonal $NaGdF_4$ (PDF card no. 01-080-8787). (D) TEM images (scale bars: 20 nm) and (E) DLS curves of PAA-coated cubic (1, red) and hexagonal (2, blue) $NaGdF_4$ NPs dispersed in water. DLS data revealed hydrodynamic diameters of 28.0 nm (PDI: 0.03) for the cubic and 27.1 nm (PDI: 0.39) for the hexagonal sample.

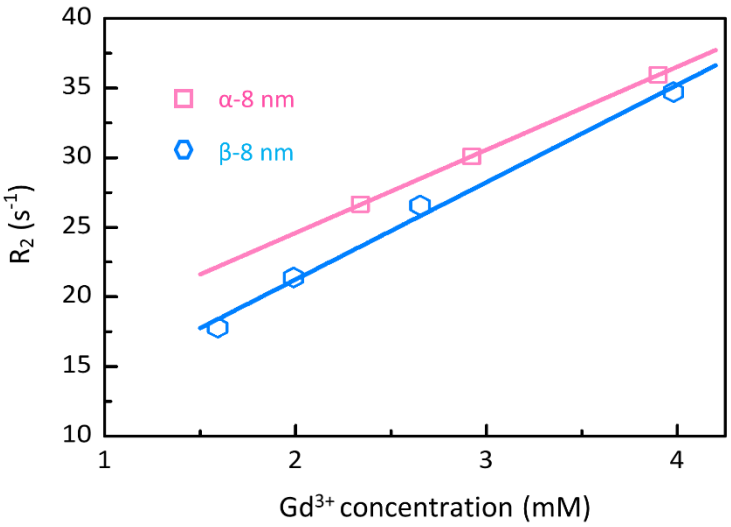

Figure S9. Relaxation rate R_2 (= $1/T_2$) of water protons plotted against the molar concentration of Gd^{3+} for cubic (α) and hexagonal (β) $NaGdF_4$ NPs coated with PAA at 3 T. Solid lines are linear fits. Red data points and fits stand for cubic NPs, while blue data points and fits stand for hexagonal NPs.

T_1-weigted images of citrate-coated $NaGdF_4$ NPs crystallized in the cubic and hexagonal phase

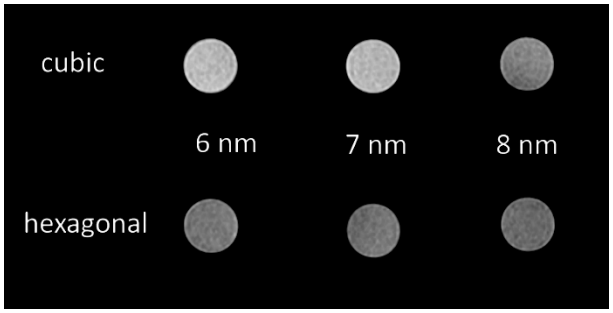

Figure S10. T_1-weigthed images of $NaGdF_4$ NPs coated with citrate of different size and crystalline phase obtained at 3 T (Gd^{3+} concentration as determined by ICP: 0.125 mM).